



OCLC FirstSearch: Display

Your requested information from your library NASA GLENN RES CTR AT LEWIS FI



Return

PENDING - Lender
Record number: 3 Total records: 3



42297881

GENERAL RECORD INFORMATION

Request Identifier: **42297881** Status: PENDING 20080425
Request Date: 20080425 Source: FSILLSTF
OCLC Number: 37266616
Borrower: **IBICT** Need Before: 20080525
Receive Date: Renewal Request:
Due Date: New Due Date:
Lenders: *NAL, MWF, IQU, HLO, AAA
Request Type: Copy

BIBLIOGRAPHIC INFORMATION

Call Number:
Title: Combustion theory and modelling /
ISSN: 1364-7830
Imprint: Bristol, UK : Institute of Physics Pub., 1997 9999
Article: Massias, A. et al "Global reduced mechanisms for methane and hydrogen combustion with nitric oxide formation..."
Volume: 3
Number: 2/6
Date: 1999
Pages: 233-257
Verified: WorldCat Availability: Alternate: Taylor & Francis, 100 Walnut St., Champlain, NY 12919
CODEN: CTMOFQ Desc: v. : Type: Serial, Internet Resource

BORROWING INFORMATION

Luana Feitosa, Ministerio da Ciencia e Tecnologia, Instituto Brasileiro de Informacao em
Ship To: Ciencia e Tecnologia (IBICT), SAS Quadra 05 Lote 06 Bl. H, CEP 70070-914 Brasilia - SD, Brazil
Bill To: same
Ship Via: In order of possibility: 1)email; 2) air mail
Electronic Delivery:
Maximum Cost: IFM - \$00
Copyright Compliance: None

Global reduced mechanisms for methane and hydrogen combustion with nitric oxide formation constructed with CSP data

A Massias†‡, D Diamantis†§, E Mastorakos† and D A Goussis†||


† Institute of Chemical Engineering and High Temperature Chemical Processes. PO Box 1414, 26500 Patra, Greece

‡ Mechanical and Aerospace Engineering Department, University of Patras, 26500 Patra, Greece

§ Chemical Engineering Department, University of Patras, 26500 Patra, Greece

Received 11 March 1998

Abstract. Reduced mechanisms for methane–air and hydrogen–air combustion including NO formation have been constructed with the computational singular perturbation (CSP) method using the fully automated algorithm described by Massias *et al.* The analysis was performed on solutions of unstrained adiabatic premixed flames with detailed chemical kinetics described by GRI 2.11 for methane and a 71-reaction mechanism for hydrogen including NO_x formation. A 10-step reduced mechanism for methane has been constructed which reproduces accurately laminar burning velocities, flame temperatures and mass fraction distributions of major species for the whole flammability range. Many steady-state species are also predicted satisfactorily. This mechanism is an improvement over the seven-step set of Massias *et al.*, especially for rich flames, because the use of HCNO, HCN and C₂H₂ as major species results in a better calculation of prompt NO. The present 10-step mechanism may thus also be applicable to diffusion flames. A five-step mechanism for lean and hydrogen-rich combustion has also been constructed based on a detailed mechanism including thermal NO. This mechanism is accurate for a wide range of the equivalence ratio and for pressures as high as 40 bar. For both fuels, the CSP algorithm automatically pointed to the same steady-state species as those identified by laborious analysis or intuition in the literature and the global reactions were similar to well established previous methane-reduced mechanisms. This implies that the method is very well suited for the study of complex mechanisms for heavy hydrocarbon combustion.

 This article features supplementary data files available from the abstract page in the online journal; see www.iop.org.

1. Introduction

The need for reduced mechanisms for the description of combustion chemistry and pollutant formation is pressing, both to improve our understanding of the relevant phenomena and to make calculations of turbulent flames with realistic chemistry feasible. The use of reduced mechanisms in flame calculations requires accurate mechanisms of small size and a wide field of application, so as to predict phenomena such as ignition, flame propagation, extinction, NO formation, etc. From the point of view of research in chemical kinetic mechanism reduction, there is a need to create mathematical tools that identify automatically the global steps, steady-state species and algebraic relations that comprise the reduced mechanism. Such tools can

|| Author to whom correspondence should be addressed. E-mail address: dagoussi@iceht.forth.gr

be used for the reduction of the long and complex mechanisms that appear continuously for hydrocarbon combustion. In this paper, we present reduced mechanisms for methane and hydrogen combustion derived from such a mathematical tool, the computational singular perturbation (CSP) method described in [1], and we discuss their range of application, as well as the insight they can offer concerning pollutant formation.

The traditional method to systematically create reduced mechanisms has been reviewed in detail in [1] and references therein. Typically, steady-state approximations and partial equilibrium assumptions are used to create a set of global steps that describe the major features of the chemistry. Various reduced mechanisms have been thus produced for methane [2–10] and other fuels [11–15].

For hydrogen, reduced mechanisms for both premixed and non-premixed flames have appeared [12, 13] and have been used extensively in turbulent flame calculations [13, 16, 17]. The absence of the prompt-NO pathway in hydrogen flames and the lack of coupling between the thermal (Zel'dovich) chemistry and the fuel-consumption reactions facilitates the construction of reduced mechanisms that also capture NO formation, such as the five-step mechanism for diffusion flames by Chen *et al* [13]. We will present here an alternative reduced mechanism for premixed combustion of hydrogen, in part to further validate CSP.

Less work has been done in creating reduced mechanisms incorporating thermal and prompt NO in hydrocarbon combustion, not least because there was no generally accepted complete set of detailed reactions for NO until recently. We could perhaps say that a degree of consensus has been achieved with the optimization of the work of Miller and Bowman [18] that culminated in various complete and extensively tested detailed mechanisms [19–21]. Recent developments to create reduced reaction sets for both methane combustion and NO formation include the six-step mechanism for lean mixtures in well-stirred reactors by Glarborg *et al* [22], an 11-step reduced mechanism for diffusion flames [23], while Chen [9] has presented a 10-step mechanism for methane ignition and combustion and a derivative 12-step set that includes NO formation for premixed and diffusion flames and well-stirred reactors. Here, we will show reduced mechanisms for premixed methane combustion that are of comparable accuracy, but use a smaller number of steps. This may be advantageous for their use in turbulent flame calculations.

The specific objectives of the present paper are to create and discuss reduced mechanisms for hydrogen and methane premixed combustion and NO formation and to further demonstrate the ability of the CSP method by constructing accurate reduced mechanisms of different sizes and for different fuels. The remainder of the paper is organized as follows. For self-consistency, certain elements of the algorithm presented in [1] are repeated in section 2. Then, the mechanisms are presented and discussed in section 3 and the paper closes with a summary of the more important conclusions.

2. The algorithm

2.1. The CSP algorithm

The construction of reduced mechanisms by CSP starts with the choice on the desired number of global steps, say S , and follows the steps outlined below. For details and the mathematical foundations of the method, the reader is referred to [1]. Here, we summarize the physical significance of CSP data and how these are used.

Step 1: the reference solution. A numerical solution of the flame structure with a suitable detailed mechanism is obtained, on which the CSP analysis is performed. It is anticipated that

the reduced mechanism will be accurate over a range of conditions close to those of the detailed kinetics solution. The exact range of the mechanism's applicability is quantified *a posteriori*.

Step 2: CSP local pointers. Given the desired number of global steps, $M = N - S$ steady-state species must be identified, where N is the total number of species in the detailed mechanism. For this purpose, CSP analysis is performed at each grid point providing the CSP pointer of each species i , $D_i(x)$, which is a function of space and takes a value between zero and unity. In physical terms, the CSP pointer is a measure of the influence of the M fastest chemical time scales on each of the species. When $D_i(x) = 1$, the i th species are completely influenced by the fastest scales and are the best candidates to be steady state. In contrast, when $D_i(x) = 0$, the fast time scales have no effect on the i th species and cannot be identified as steady state.

Step 3: integrated pointers. The local pointer $D_i(x)$ is integrated across the flame using the local species net production rate and species mole fraction as a weighting factor, to give an 'integrated CSP pointer' for each species:

$$I_i = \frac{1}{L} \int_0^L D_i(x) \frac{|q_i(x)|}{|q_i|_{\max} X_i(x)} dx \quad (1)$$

where $|q_i|$ is the net species production rate, $|q_i|_{\max}$ is the corresponding maximum inside the calculation domain of length L and X_i is the species mole fraction. In contrast to the CSP pointers, the scalars I_i can take any value between zero and infinity. As discussed in [1], the weighting by the mole fraction is consistent with the traditional criterion of taking low-concentration species as the steady-state ones. The quantities I_i for each species are ordered and the $N - M$ species with the lowest values are taken as major (non-steady-state) species. The M species with the largest values are identified as steady-state species. We will discuss in section 3.1.1 such ordered lists that show which species would be treated as steady state for various mechanisms. It will become evident that equation (1) points to major species consistent with our intuition and the choices made in previous literature of reduced mechanisms.

Step 4: fast reaction identification. The rate of each elementary reaction is integrated along the flame. The reactions that consume the steady-state species (step 3) and exhibit the largest integrated rate are selected and deemed the 'fast' reactions (the rest are 'slow'). For M steady-state species, M fast reactions are selected.

Step 5: global reactions. Based on the results of steps 3 and 4, the stoichiometry and rates of the global reactions are compiled following [1, 24]. The reduced mechanism consists of the global steps involving the major species and the corresponding global rates, which are expressed as linear combinations of the 'slow' elementary rates. These rates depend, of course, on all species, steady state *and* non-steady state. The former are calculated from the solution of a system of steady-state algebraic relations with the 'inner iteration' procedure.

Step 6: truncations. The accuracy of the reduced mechanism constructed by steps 1–5 above might not be the optimum one. Frequently, abnormally high concentrations are encountered for some steady-state species, which might result in low accuracy. This problem is resolved by comparing the relative contributions of each elementary reaction to the total production rate for the species from both the reduced and detailed mechanisms. If large discrepancies exist, the corresponding elementary rates are truncated from the steady-state relations [25, 26]. Typically, only two to three truncations are necessary (section 3.1.2).

If step 3 were missing, the sequence of steps 1–5 would create ‘local’ reduced mechanisms [1]. The integrated pointers, however, provide an objective way to identify species that can be treated as steady state throughout the computational domain. Hence the construction of ‘global’ reduced mechanisms is possible. Steps 1–5 above are fully automated in the computer code S-STEP [1], which takes as input the detailed kinetics solution and the user-defined number of global steps. It produces the reduced stoichiometry, global reaction rates and algebraic relations for the steady-state species. Typically, this code takes a few minutes of CPU time on a current workstation.

2.2. Detailed mechanisms and flame solutions

The detailed mechanism GRI 2.11 [20] was used here as the basis for the construction of the reduced methane mechanisms. This mechanism has been optimized against experimental data at low and high pressures for ignition delays, perfectly stirred reactors and laminar flames and is considered to be one of the most up-to-date detailed mechanisms concerning methane combustion and nitrogen oxides formation [20]. It consists of 279 reactions with 49 species and includes C_2 species, prompt and thermal NO, and nitrous oxide chemistry. The hydrogen mechanism we used is presented in the appendix [27]. It includes nitrogen oxides formation and consists of 71 reactions with 18 species. For both fuels, solutions for unstrained adiabatic premixed flames have been obtained with the code RUN-IDL, developed by Rogg [28]. Unless otherwise noted, all flames were computed at an initial temperature of 300 K and a constant pressure of 1 bar.

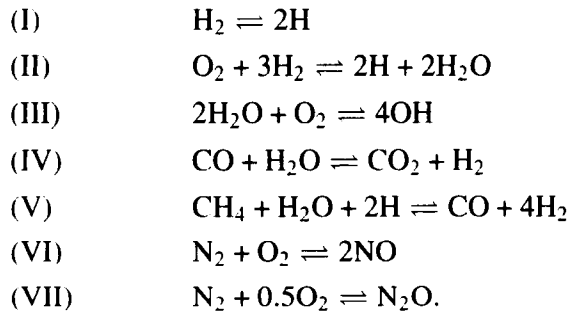
3. Results and discussion

In this section we present and discuss the various reduced mechanisms constructed for methane and hydrogen flames. We discuss aspects of the reduction procedure by examining in detail the methane mechanisms. The seven-step methane mechanism is taken from [1] and is compared here with a new 10-step one. The strengths and limitations of each reduced set are emphasized.

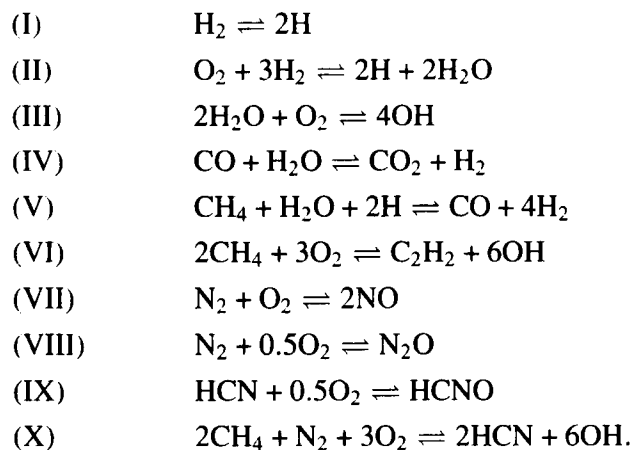
3.1. Seven-step and 10-step reduced mechanisms for methane

3.1.1. Integrated CSP pointers. We present first the integrated pointers (I_i) for all species appearing in the detailed mechanism. The lists in tables 1 and 2 are the integrated CSP pointers presented in descending order for the seven- and 10-step mechanisms, respectively. The species low in the list are taken as major ones, while those early in the list (i.e. with high value of integrated pointer) are treated as steady state. Tables 1 and 2 are different because the integrated pointers are not a unique property of the detailed chemistry solution, but also depend on the desired number of global steps. The CSP pointers denote the angle of the species’ axes with respect to the manifold, along which the solution (trajectory) evolves. The species producing the largest pointers have their axes the most perpendicular to the manifold. Since this manifold depends on the number of global steps, the pointer value changes with the **dimension of the reduced mechanism**. **The mechanism is constructed by selecting as major species the last M_{ms} in the list, where M_{ms} is the desired number of global steps plus the number of elements appearing in the detailed mechanism (in the case of GRI 2.11 and a 10-step reduced mechanism, $M_{ms} = 10 + 5 = 15$).** It is possible to bypass this ordering, if one wishes to treat a specific species as major in order to ensure its more accurate calculation.

3.1.2. *The reduced mechanisms.* The solution for $\phi = 1.0$ was selected for the construction of the seven-step reduced mechanism [1] and the resulting global steps are repeated below to facilitate comparison with the new 10-step reduced mechanism:



The mechanism was created automatically by S-STEP, with only one truncation in the steady-state relations. The 10-step mechanism was constructed on the basis of the ordering of table 2, but for $\phi = 1.2$, chosen so that a C₂ species appears in the major species set which is anticipated to improve predictions for rich flames. The resulting global steps are given below†:



A comparison between the two reduced mechanisms shows that the seven-step mechanism is a subset of the 10-step one, as reactions I–V and VII–VIII of the 10-step one contain the seven-step mechanism. The first six global reactions in the 10-step mechanism describe methane combustion and the rest nitrogen chemistry. The 10-step mechanism contains the additional major species C₂H₂, HCN and HCNO. It was not surprising that the first two should appear in a reduced mechanism valid for rich flames [9, 22, 23], but the identification of HCNO as a major species was not evident. Finally, note that N₂O appears in both mechanisms as a major species, in contrast to other reduced mechanisms [9, 22]. Again, this outcome of the CSP analysis deserves some discussion, which is facilitated after the presentation of results which is given next.

3.1.3. *Results.* Both mechanisms are in excellent agreement with GRI 2.11 for laminar burning velocities for all equivalence ratios between the flammability limits (see figure 1). Figure 2 shows the excellent prediction of the carbon monoxide profile along the flame. The agreement for all other major species is at least as good as for the monoxide, to the point that most curves are indistinguishable on the graphs. Very small differences may be seen for the peaks of CO (figure 2), H and OH (figure 3), but it is evident that both reduced mechanisms

† The rates and steady-state relations are given in a supplementary data file available from the abstract page in the online journal: see www.iop.org.

Table 1. Continued.

	$\phi = 0.5$	$\phi = 0.8$	$\phi = 1.0$	$\phi = 1.2$	$\phi = 1.4$					
28	HCN	0.825E+03	HNCO	0.271E+02	CH ₃ OH	0.131E+02	CH ₂	0.126E+02	C ₂ H ₅	0.324E+02
29	C ₂ H ₅	0.810E+03	C ₂ H ₂	0.220E+02	HNCO	0.107E+02	HO ₂	0.678E+01	CH ₃ OH	0.252E+02
30	H ₂ O ₂	0.200E+03	HCO	0.192E+02	C ₂ H ₂	0.554E+01	HNCO	0.675E+01	NO	0.190E+02
31	CH ₃ OH	0.103E+03	CH ₃ OH	0.141E+02	HO ₂	0.489E+01	CH ₂ O	0.138E+01	HO ₂	0.188E+02
32	H	0.381E+02	HO ₂	0.656E+01	C ₂ H ₄	0.191E+01	C ₂ H ₂	0.129E+01	O	0.166E+02
33	C ₂ H ₆	0.320E+02	HCN	0.456E+01	C ₂ H ₆	0.129E+01	C ₂ H ₄	0.117E+01	CH ₂ CO	0.136E+02
34	C ₂ H ₄	0.247E+02	C ₂ H ₄	0.372E+01	CH ₂ O	0.108E+01	C ₂ H ₆	0.116E+01	OH	0.455E+01
35	CH ₂ O	0.145E+02	C ₂ H ₆	0.259E+01	HCN	0.769E+00	O	0.888E+00	CH ₂ O	0.240E+01
36	CH ₃	0.132E+02	CH ₂ O	0.182E+01	CH ₃	0.387E+00	CH ₃	0.312E+00	H	0.169E+01
37	HO ₂	0.106E+02	H	0.782E+00	O	0.306E+00	H	0.293E+00	C ₂ H ₆	0.153E+01
38	O	0.687E+01	CH ₃	0.739E+00	H	0.306E+00	OH	0.286E+00	C ₂ H ₄	0.814E+00
39	OH	0.381E+01	O	0.377E+00	OH	0.173E+00	HCN	0.237E+00	CH ₃	0.507E+00
40	H ₂	0.221E+01	OH	0.294E+00	CH ₄	0.501E-01	N ₂ O	0.667E-01	C ₂ H ₂	0.618E-01
41	HCNO	0.219E+01	CH ₄	0.700E-01	NO	0.369E-01	CH ₄	0.423E-01	HCN	0.312E-01
42	CH ₄	0.683E+00	H ₂	0.366E-01	H ₂	0.130E-01	NO	0.192E-01	CH ₄	0.303E-01
43	N ₂ O	0.100E+00	N ₂ O	0.347E-03	N ₂ O	0.609E-02	H ₂	0.669E-02	O ₂	0.878E-02
44	CO	0.280E-02	CO	0.199E-03	CO	0.131E-03	O ₂	0.455E-03	H ₂	0.423E-02
45	H ₂ O	0.693E-04	H ₂ O	0.287E-04	O ₂	0.486E-04	CO	0.104E-03	CO ₂	0.310E-03
46	O ₂	0.222E-04	O ₂	0.101E-04	H ₂ O	0.307E-04	CO ₂	0.426E-04	H ₂ O	0.167E-03
47	CO ₂	0.236E-06	CO ₂	0.894E-06	CO ₂	0.620E-05	H ₂ O	0.271E-04	CO	0.127E-04
48	N ₂	0.349E-12	N ₂	0.170E-11	N ₂	0.835E-11	N ₂	0.291E-10	N ₂	0.109E-10
49	AR	0.100E-60	AR	0.100E-60	AR	0.100E-60	AR	0.100E-60	AR	0.100E-60

↑

Table 2. Continued.

	$\phi = 0.5$	$\phi = 0.8$	$\phi = 1.0$	$\phi = 1.2$	$\phi = 1.4$
28	H ₂ O ₂	HCO	HO ₂	HNCO	NO
29	CH ₃ OH	CH ₃ OH	C ₂ H ₄	CH ₂ O	HO ₂
30	H	HO ₂	C ₂ H ₂	CH ₂ CO	O
31	C ₂ H ₆	C ₂ H ₆	C ₂ H ₆	C ₂ H ₆	CH ₂ CO
32	C ₂ H ₄	HCN	CH ₂ O	C ₂ H ₄	OH
33	CH ₂ O	CH ₂ O	HCN	O	HNCO
34	HCN	H	CH ₃	CH ₃	CH ₂ O
35	CH ₃	CH ₃	O	H	H
36	HO ₂	C ₂ H ₄	H	OH	C ₂ H ₆
37	O	O	OH	HCN	C ₂ H ₄
38	OH	OH	CH ₂ CO	C ₂ H ₂	CH ₃
39	H ₂	CH ₂ CO	CH ₄	N ₂ O	N ₂ O
40	CH ₂ CO	CH ₄	NO	CH ₄	HCN
41	CH ₄	H ₂	H ₂	NO	CH ₄
42	CO	HCNO	N ₂ O	H ₂	C ₂ H ₂
43	H ₂ O	N ₂ O	HCNO	HCNO	H ₂
44	HCNO	CO	O ₂	O ₂	O ₂
45	O ₂	H ₂ O	CO	CO	H ₂ O
46	N ₂ O	O ₂	H ₂ O	CO ₂	CO
47	CO ₂	CO ₂	CO ₂	H ₂ O	CO ₂
48	N ₂	N ₂	N ₂	N ₂	N ₂
49	AR	AR	AR	AR	AR

↑

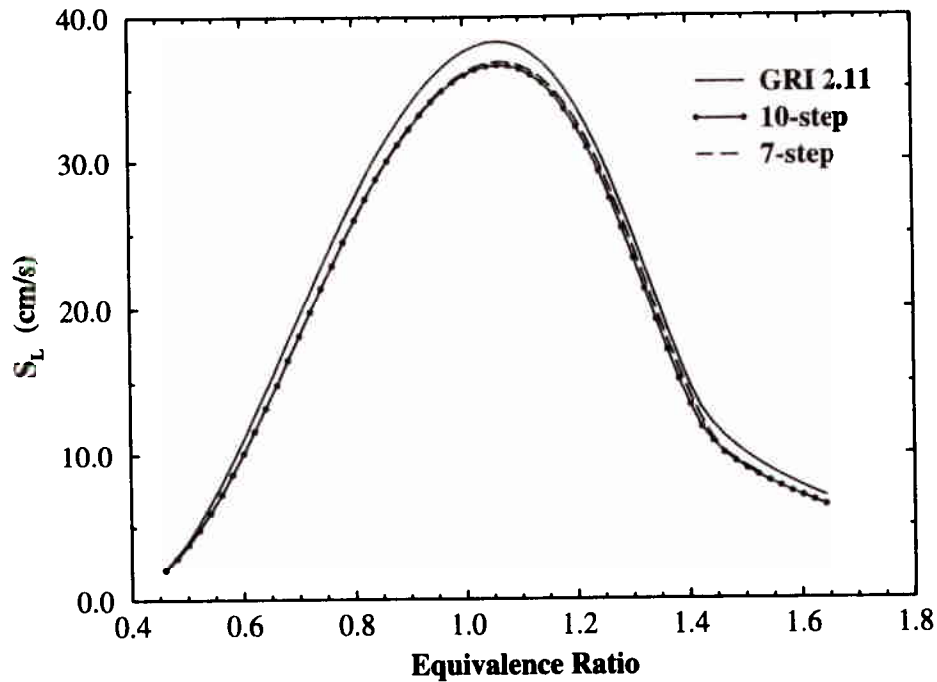


Figure 1. Laminar burning velocity as a function of equivalence ratio for premixed flames.

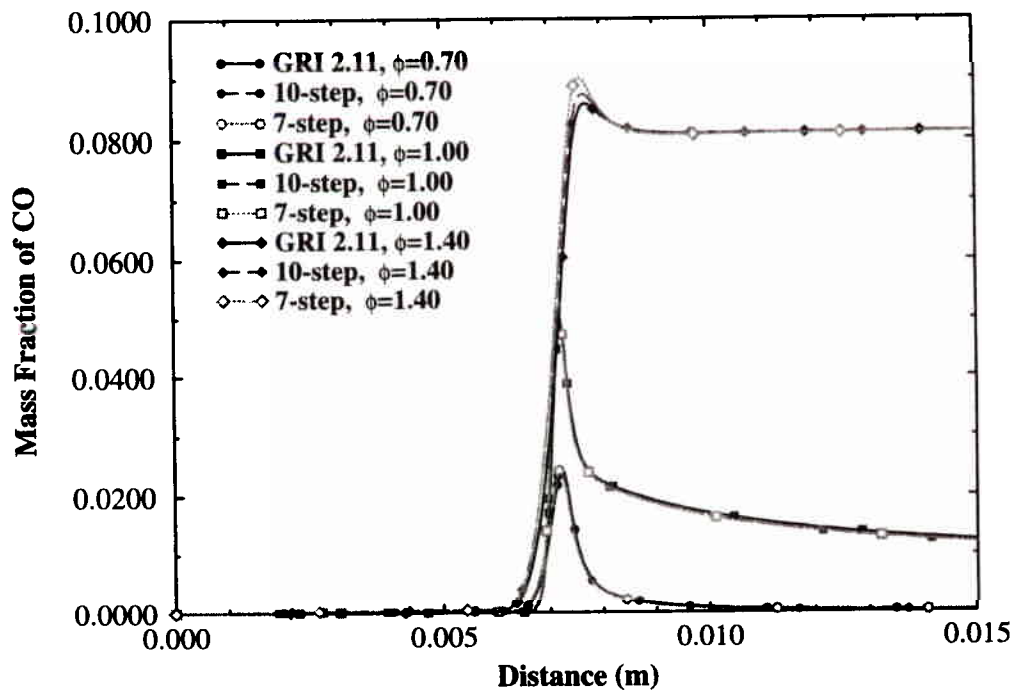


Figure 2. CO mass fraction for premixed methane flames for three different equivalence ratios. (This figure can be viewed in colour in the electronic version of the article; see www.iop.org)

perform very well. The fact that a reduced mechanism constructed at one equivalence ratio is also so successful at lean and rich combustion demonstrates the ability of the CSP method.

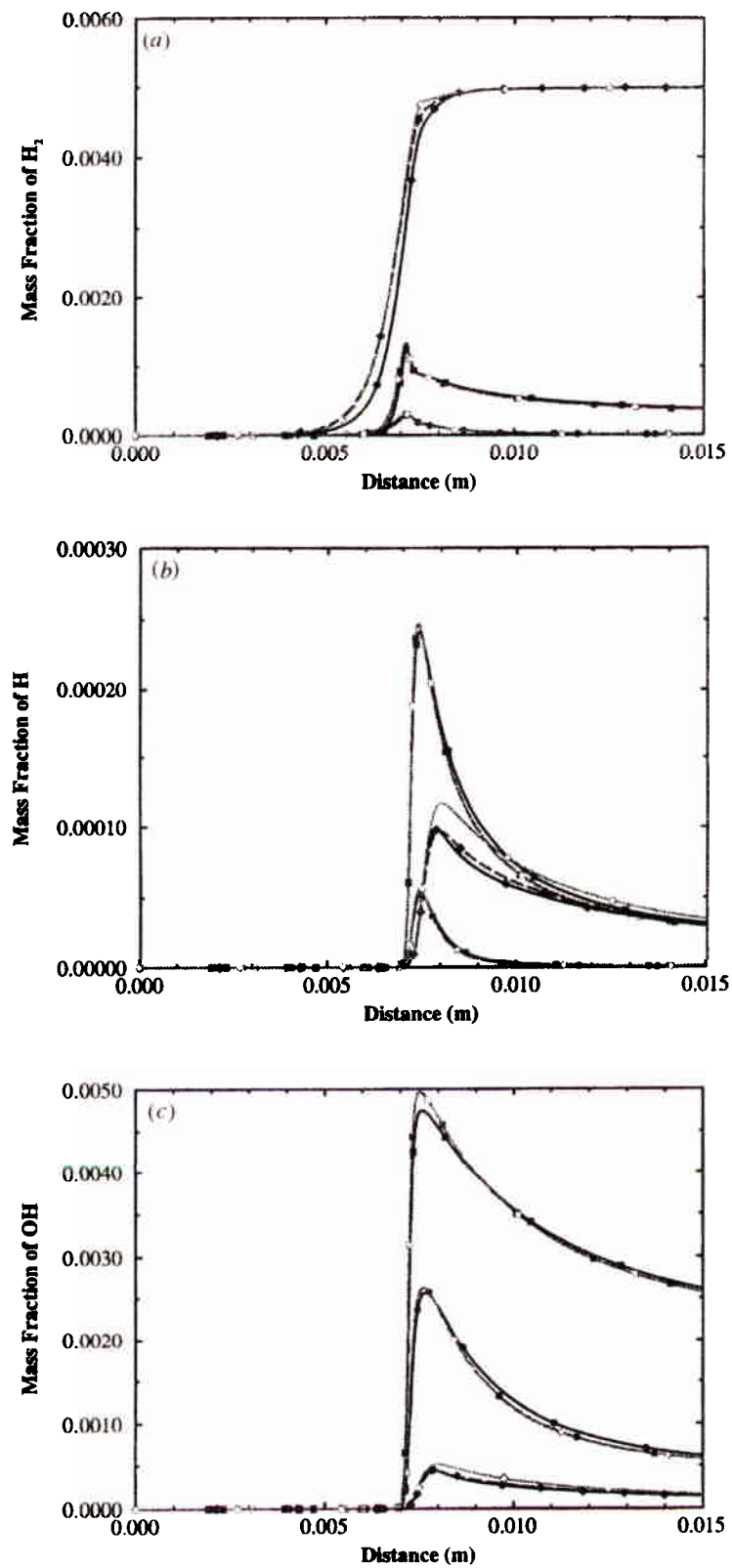


Figure 3. Mass fraction, Y , of (a) H_2 , (b) H , (c) OH , (d) O , (e) CH_3 and (f) CH_2CO for premixed methane flames for three different equivalence ratios. The first three are major and the last three are steady-state species in both reduced mechanisms. Symbols and curves as in figure 2.

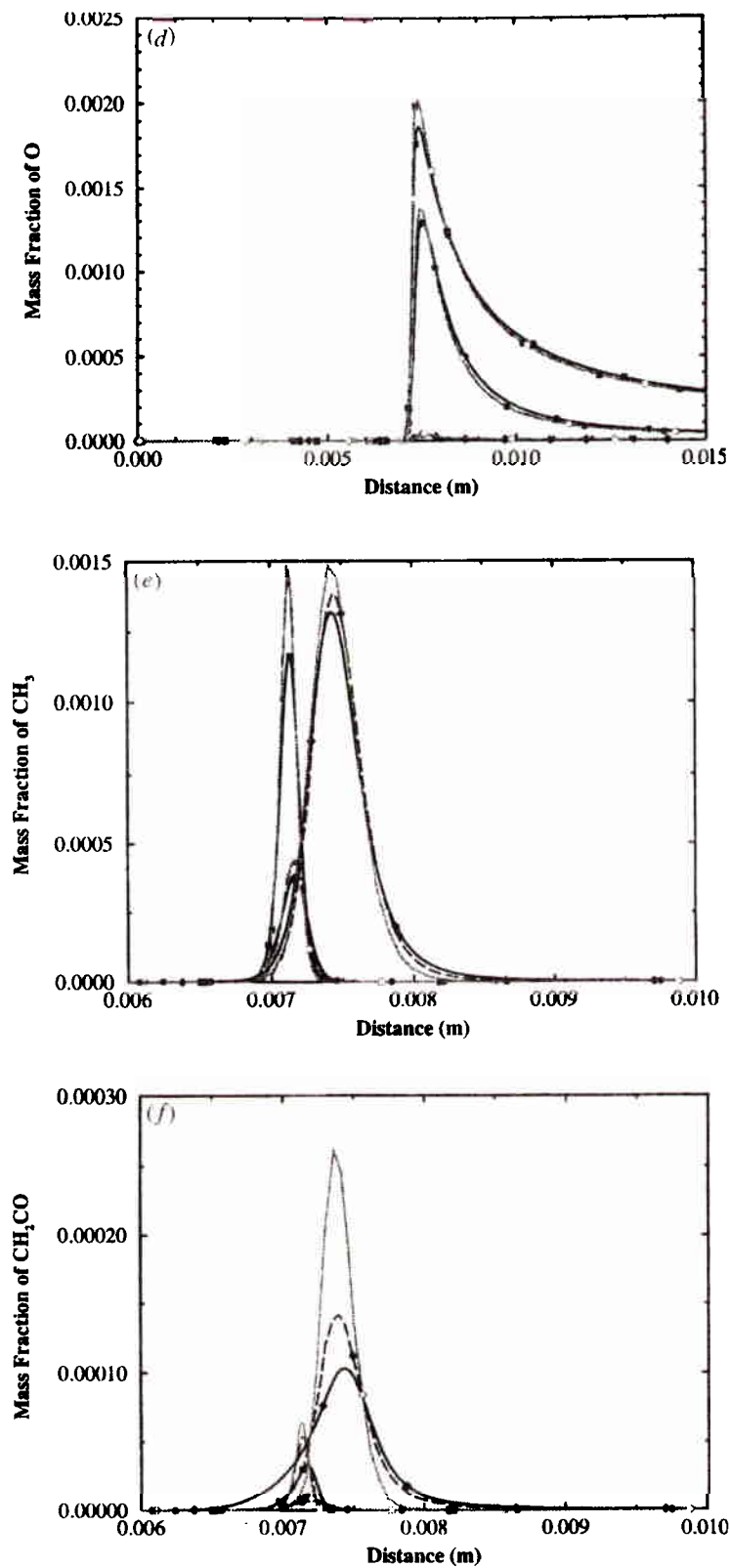


Figure 3. Continued.

The agreement between the reduced mechanisms and GRI 2.11 is also very good for nitrogen-containing major species. Figure 4 shows that the NO at the end of the computational

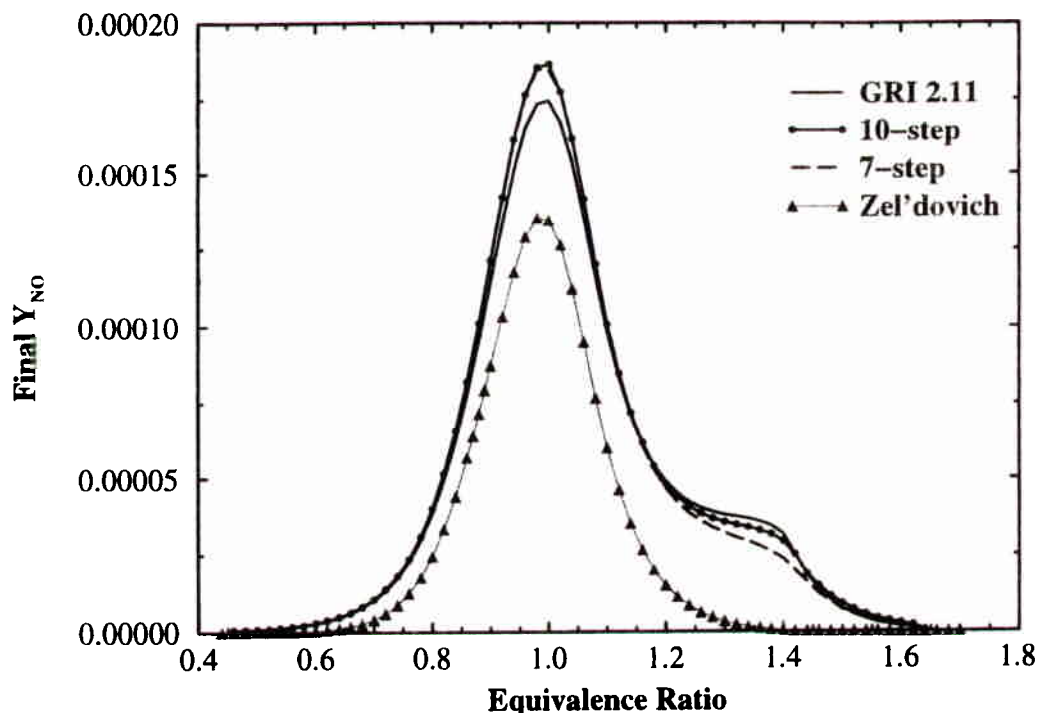


Figure 4. NO mass fraction at $x = 30$ mm as a function of the equivalence ratio. Includes data from a GRI 2.11 mechanism with all nitrogen chemistry removed except the Zel'dovich reactions.

domain (at $x = 30$ mm, corresponding to about 23 mm from the main reaction zone) is reproduced very well by the seven-step mechanism, with a small deviation beginning after about $\phi = 1.2$, while the 10-step mechanism gives excellent predictions even for very rich flames. The peak NO occurs at stoichiometry and the error between the reduced and detailed mechanisms is around 5%, which is considered very small. Profiles of N_2O and NO across the flame are also very well reproduced (figure 5) by both mechanisms for lean and stoichiometric flames. The slight inaccuracy of the seven-step mechanism for rich flames is explained by the underprediction of prompt NO by this mechanism (figure 5(b), $\phi = 1.4$).

The relative importance of thermal over prompt NO is shown more clearly in figure 4 which includes predictions with a version of the GRI 2.11 mechanism with all nitrogen chemistry removed, except for the Zel'dovich reactions. (The reaction rate coefficients appearing in GRI for the thermal-NO reactions are the same as those of the Zel'dovich mechanism [29].) It is evident that for stoichiometric flames the Zel'dovich mechanism accounts for about 80% of the NO formed. The thermal contribution becomes negligible for flames leaner than 0.6 and richer than 1.3, with significant NO formed by the prompt mechanism and through N_2O . It is clear that an accurate prediction of NO cannot be made based only on the Zel'dovich mechanism.

Differences between the seven- and 10-step mechanisms are also shown in figure 6. The species HCN, C_2H_2 and HCNO are taken as steady state in the seven-step mechanism and as major species in the 10-step one, and this results in a much better prediction by the latter. In general, our experience shows that if a species is taken as major it is predicted more accurately, and the accuracy of approximation of some steady-state species increases with the number of steps used (see, for example, the equal accuracy in the two reduced mechanisms for the steady-state species O and CH_3 in figures 3(d) and (e), but the better approximation of CH_2CO by the 10-step mechanism in figure 3(f)). Carrying C_2H_2 , HCN and HCNO as major species

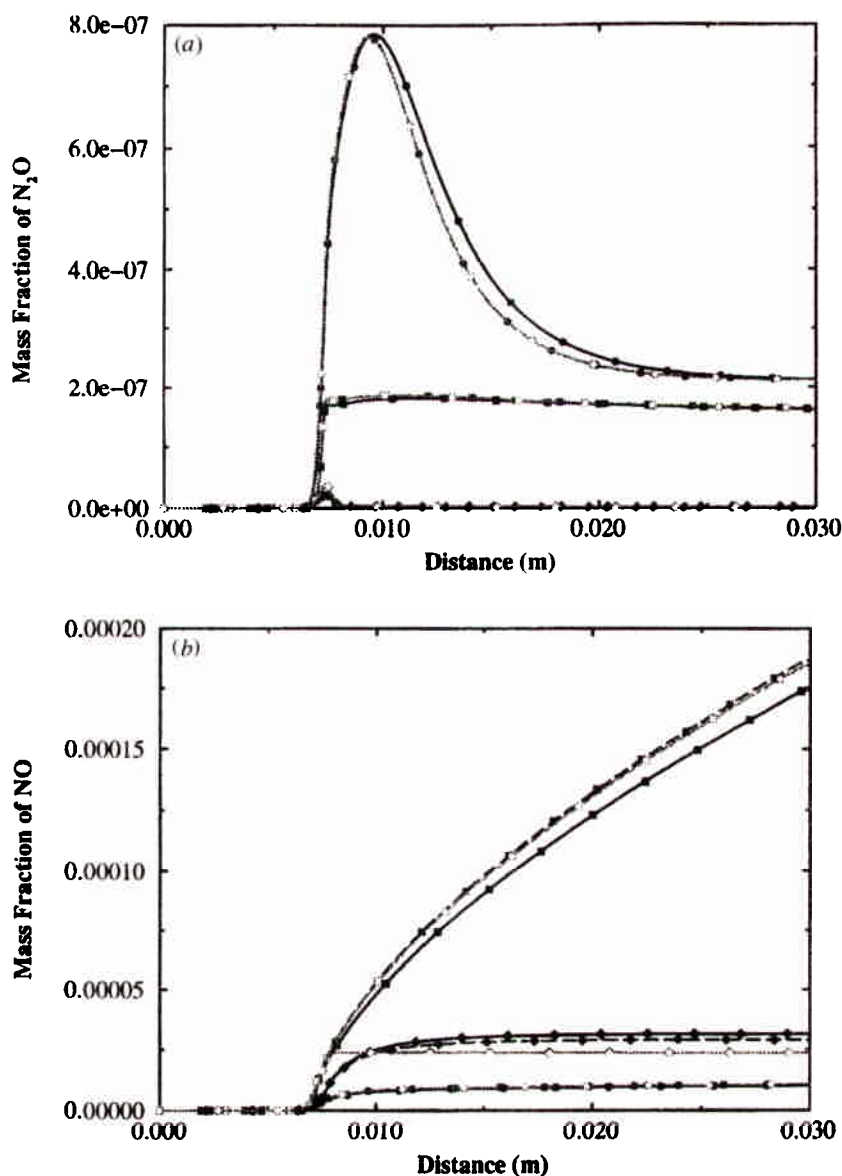


Figure 5. Mass fractions of (a) N_2O and (b) NO for premixed methane flames for three different equivalence ratios. Symbols and curves as in figure 2.

in the 10-step mechanism helps, we believe, in the somewhat better prediction of prompt NO in rich flames.

Finally, as a check on the applicability of the reduced mechanisms for various operating conditions, figure 7 shows that the increase of the laminar burning velocity with the initial mixture temperature is very accurately captured.

3.1.4. Discussion. A comparison of our reduced mechanisms with others found in the literature is given below. First, reactions I–III and V in the 10-step mechanism form the mechanism of Peters and co-workers [2, 6] and, after some manipulations, the mechanism of Bilger and co-workers [4, 5]. It is clear that we have reproduced with CSP, in an automatic manner, these well established mechanisms produced by traditional approaches and this gives credence to the present method. Second, a comparison with the diffusion-flame 11-step reduced

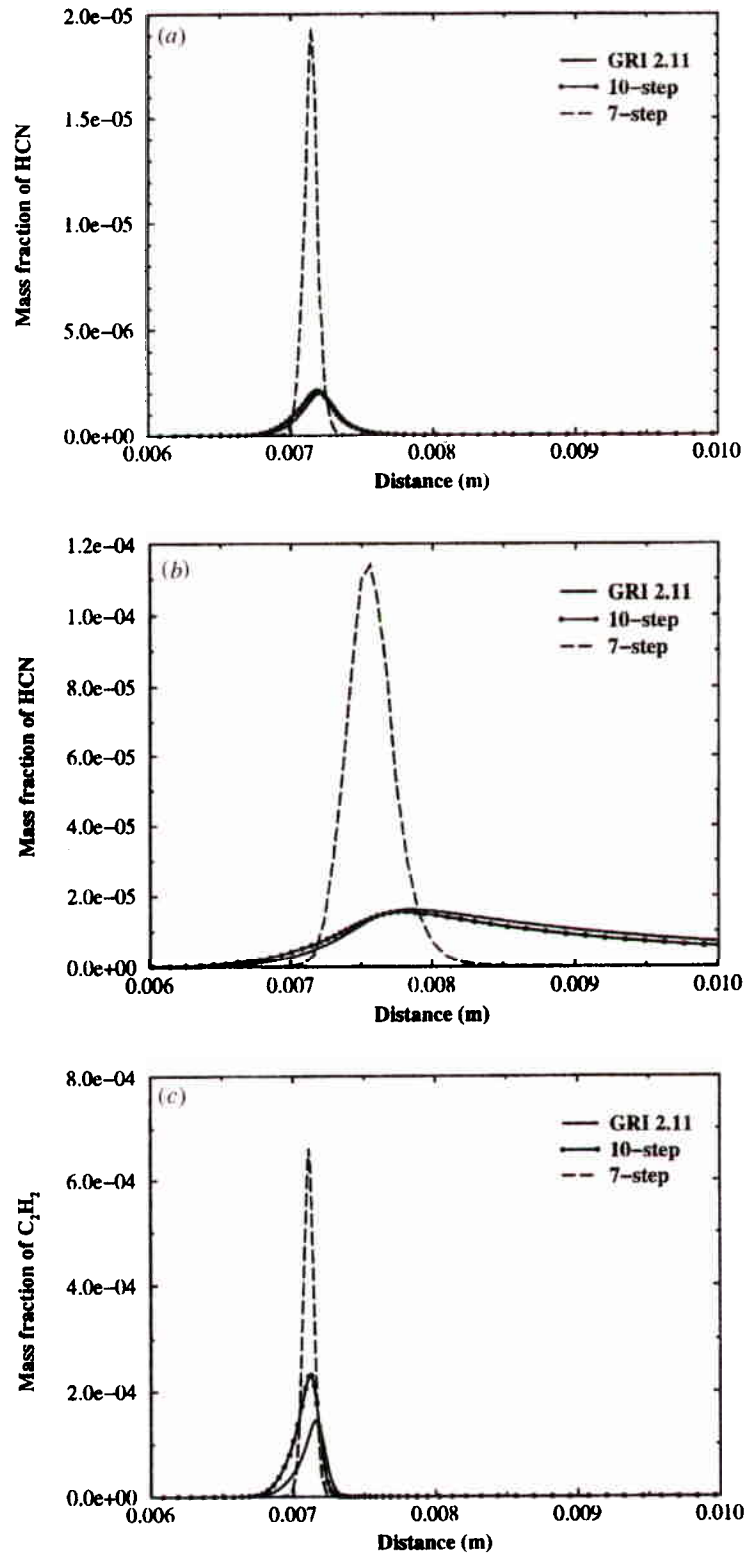


Figure 6. Mass fractions of HCN, C_2H_2 and HCNO for premixed methane flames for $\phi = 1.0$ (a), (c), (e) and $\phi = 1.4$ (b), (d), (f). These species are steady state in the seven-step mechanism [1] and major in the 10-step mechanism.

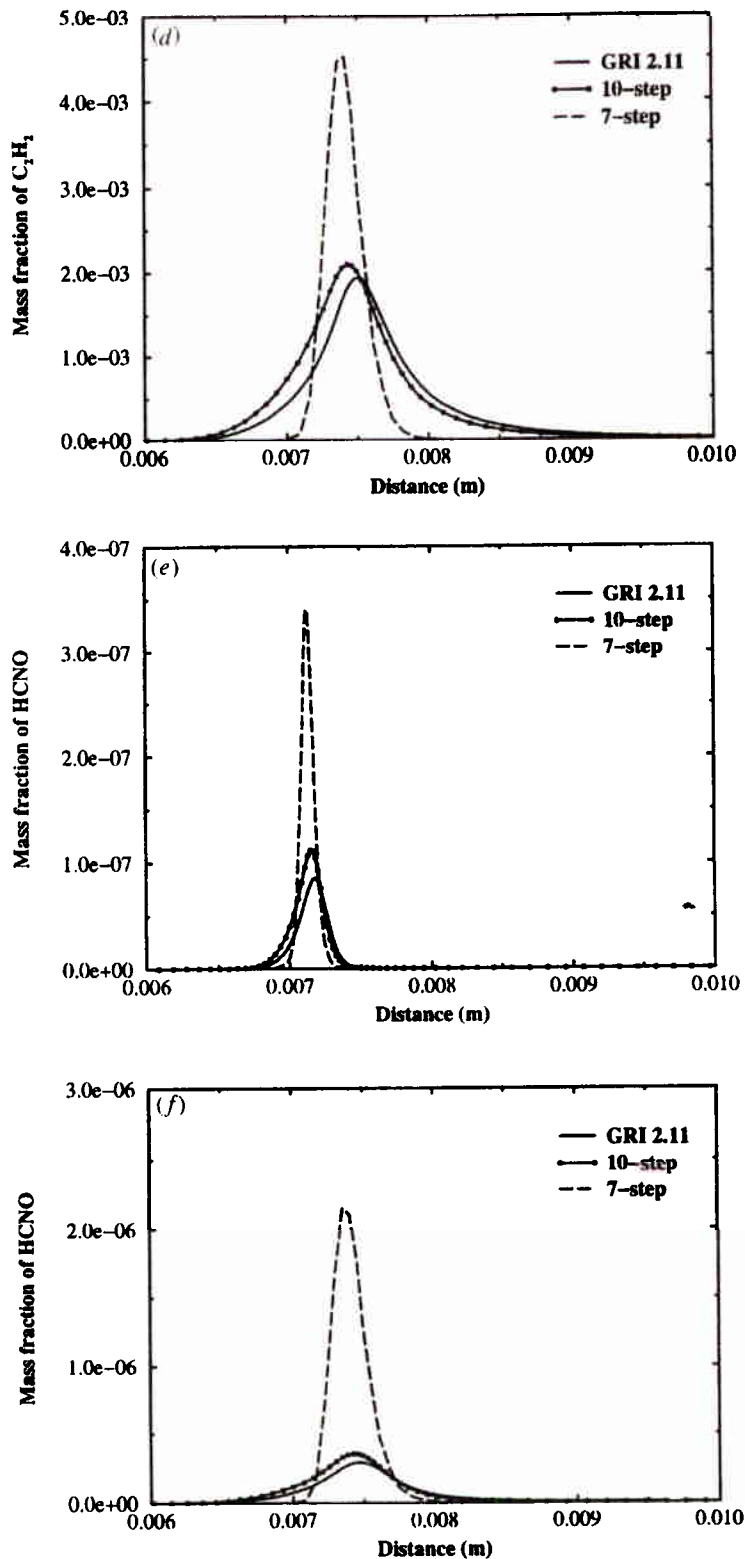


Figure 6. Continued.

mechanism of Hewson and Bollig [23] shows that we have kept N_2 , HCN, N_2O and NO as major species important to nitrogen chemistry, while these authors also use NH_3 and NO_2 , and

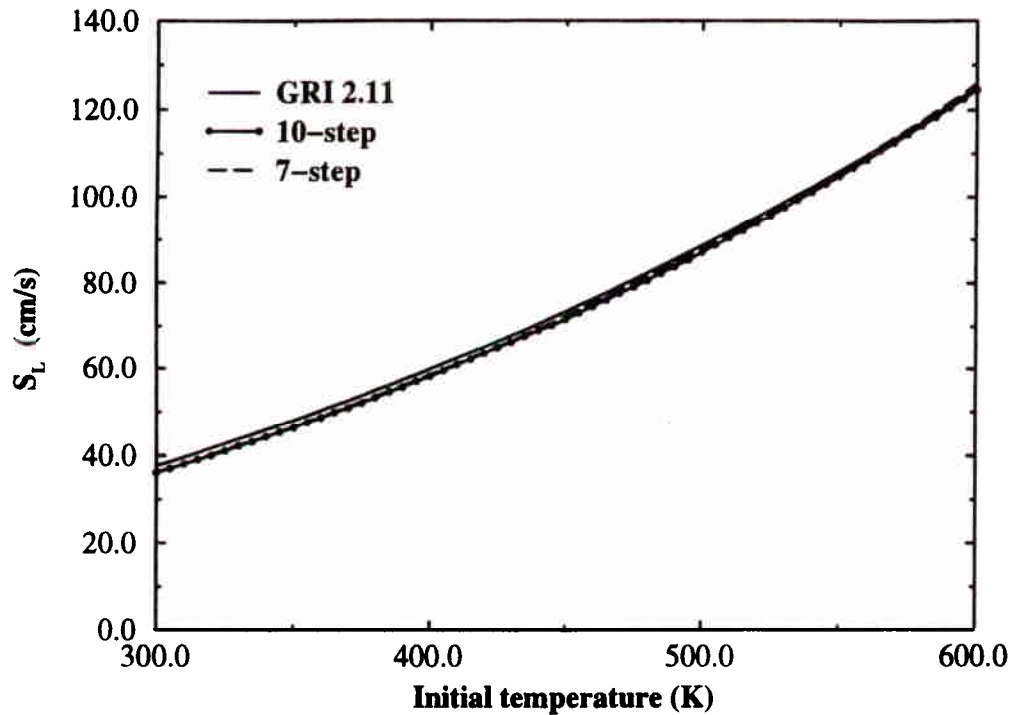


Figure 7. Laminar burning velocity of methane premixed flames as a function of initial temperature.

HNCO rather than HCNO. The overall similarity between the mechanisms and the excellent behaviour of the 10-step reduced mechanism for rich combustion suggests that our set could also be used for diffusion flames.

Further examination of the integrated CSP pointers is very instructive. It was shown in [1] how different mechanisms (i.e. with a different number of steps) can be constructed by CSP and here we discuss the different species that would participate in mechanisms of equal dimension, but constructed at different ϕ . Let us follow, by way of example, the evolution of the position of C₂H₂ from lean to rich combustion in a 10-step reduced mechanism (table 2). For $\phi = 0.5$, this species occupies position 25 (i.e. 10-species 'deep' into the steady-state ones from the limiting line of $49 - 5 - 10 = 34$) and first becomes a major species at about $\phi = 1.1$. At richer flames, it is clear that C₂H₂ is a major species, consistent with other reduced mechanisms [9, 23] and the fact that rich combustion proceeds through a C₂ pathway [30]. As another example, note that HCN and CH₃ could or could not be taken as major species since their positions lie close to the limiting line. However, they are definitely major species for rich flames (column for $\phi = 1.4$). Finally, consider the case of N₂O, which appears as a major species for all ϕ . Note the very small mass fraction of this species throughout the flame (figure 5). Based on this observation, the 'traditional' criterion [1] would deem N₂O as steady state. The fact that N₂O is a major species in the present mechanisms does not imply that the N₂O pathway contributes more than the prompt or thermal NO, but rather that for these low-pressure flames the N₂O chemistry subset is slow and insignificant [31], and so N₂O is more like an inert than a reactive species in what concerns the rest of the flame. This provides an explanation for the occurrence of species with low-mass fractions in the major-species part of the CSP list. The fact that the steady-state approximation for N₂O is not valid has also been concluded by Lindstedt and Selim [32] by comparative testing of reduced mechanisms that use this approximation and others that do not, perhaps a more time-consuming effort compared to the examination of the integrated pointers performed here.

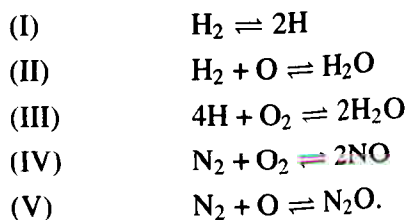
It is interesting to observe the evolution of NO in tables 1 and 2. For flames away from stoichiometry, NO lies in the steady-state part of the list. This, for example, implies that were we to construct a mechanism at, say, $\phi = 0.5$, NO would be calculated from algebraic relations in the 'inner iteration' part of the solution procedure [1, 28]. Although in practice it would perhaps be unwise to construct such a mechanism if emphasis were needed on the accurate prediction of NO, treating NO as steady state for very lean or very rich flames is consistent with the relatively low importance of the Zel'dovich mechanism at lean and rich flames (figure 4). The thermal mechanism continuously produces NO in the post-flame region and so it is impossible to consider NO as steady state in high-temperature flames where this mechanism is active. Indeed, the CSP pointers show that NO is a major species for ϕ around unity (table 2). In contrast, the prompt mechanism produces NO only in a narrow region inside the flame, with the profile of NO resembling a step function (figure 5(b)) going from zero before the flame to a constant level right after the reaction zone. Such behaviour is not inconsistent with the steady-state assumption since the net creation rate of NO is virtually zero for most of the calculation domain.

In this section, we have presented a new reduced mechanism for methane premixed flames that is very accurate for the prediction of flame speeds, flame temperatures and pollutant formation for the whole flammable range of equivalence ratio. The advantage of the new mechanism is that it contains C_2H_2 and makes a better prediction of NO for rich flames, which suggests that it may also be valid for diffusion flames. All pathways of NO formation present in GRI 2.11 (thermal, prompt, N_2O) have been captured adequately. The success of a single reduced mechanism in flames with various equivalent ratios and initial temperatures to reproduce all major species and pollutants, indicates the ability of CSP to create highly accurate reduced mechanisms.

In general, the CSP-based automatic major species selection is consistent with the choices made by other investigators. Both the discussion above and the very good results obtained by the reduced mechanisms suggest that the integrated pointer criterion works very well and reflects what we know about the chemistry. Lists such as in tables 1 and 2 may offer an additional way to reaction path analysis and sensitivity analysis to help with the comprehension of hydrocarbon chemistry. The consistency of the CSP-based observations with the literature indicates that the method's potential will prove very useful for large and complicated mechanisms, such as for example for heavy hydrocarbon combustion, soot formation or atmospheric pollution chemistry.

3.2. Five-step reduced mechanism for H_2 -air flames

A reduced mechanism for hydrogen premixed combustion is presented here to further show the potential of the CSP method. As for the reduced mechanisms for methane discussed previously, the major species that appear have been selected by examination of the CSP pointers at $\phi = 1.2$. The global steps are given below†:



† The rates and steady-state relations are given in a supplementary data file available from the abstract page in the online journal; see www.iop.org.

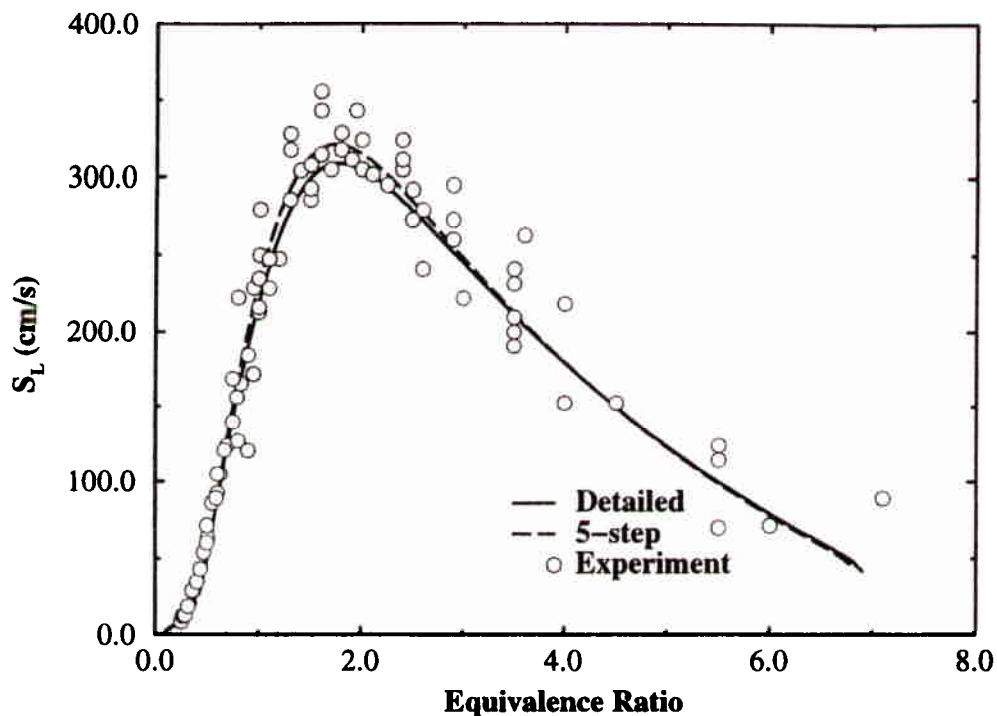


Figure 8. Laminar burning velocity as a function of the equivalence ratio for hydrogen premixed flames. Experimental data from [12].

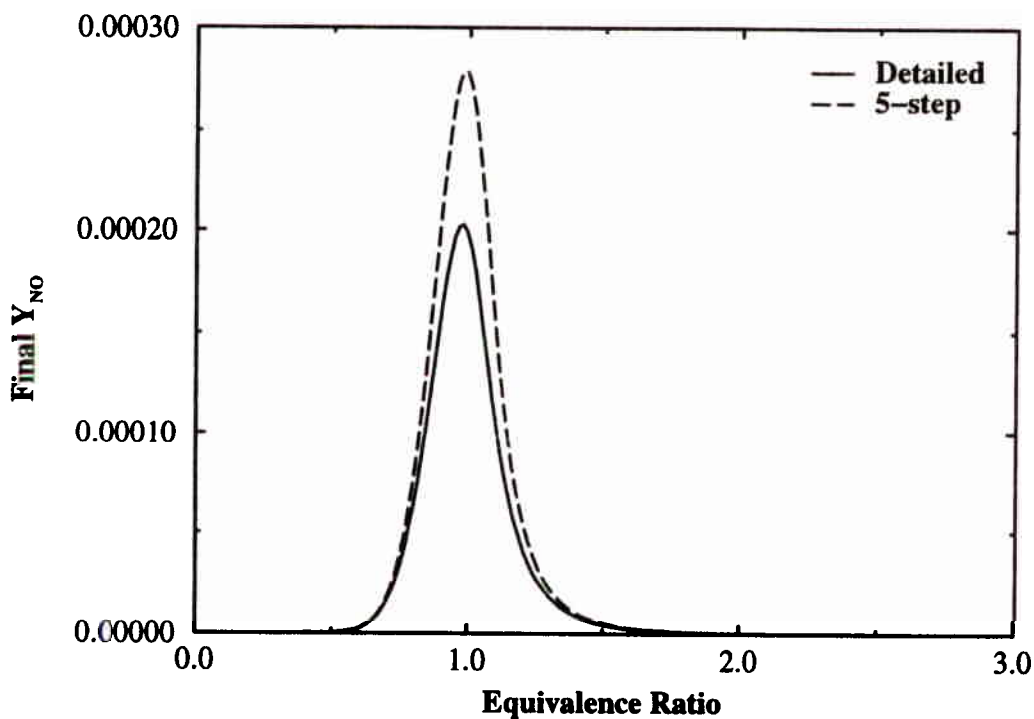


Figure 9. NO mass function at $x = 30$ mm as a function of the equivalence ratio for hydrogen premixed flames.

Steps (I) and (III) form, after a straightforward linear combination, the two-step mechanism of Mauss *et al* [12], while a comparison with the five-step reduced mechanism of Chen

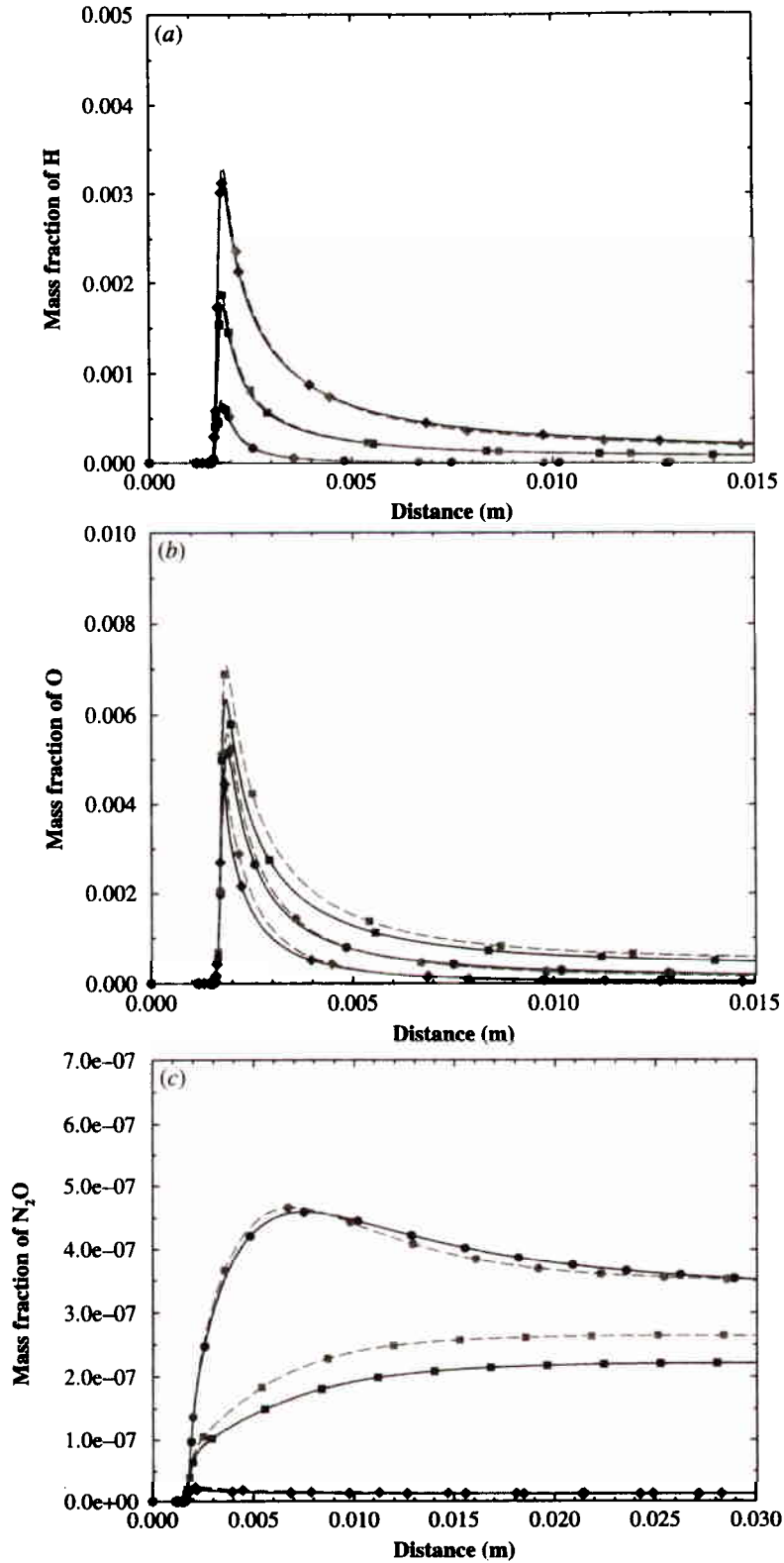


Figure 10. Mass fractions of H, O and N_2O for hydrogen premixed flames: (a) Y_H , (b) Y_O , (c) Y_{N_2O} . Full curves, detailed mechanism; broken curves, reduced mechanism; circles, $\phi = 0.7$; squares, $\phi = 1.0$; diamonds, $\phi = 1.4$.

(This figure can be viewed in colour in the electronic version of the article; see www.iop.org)

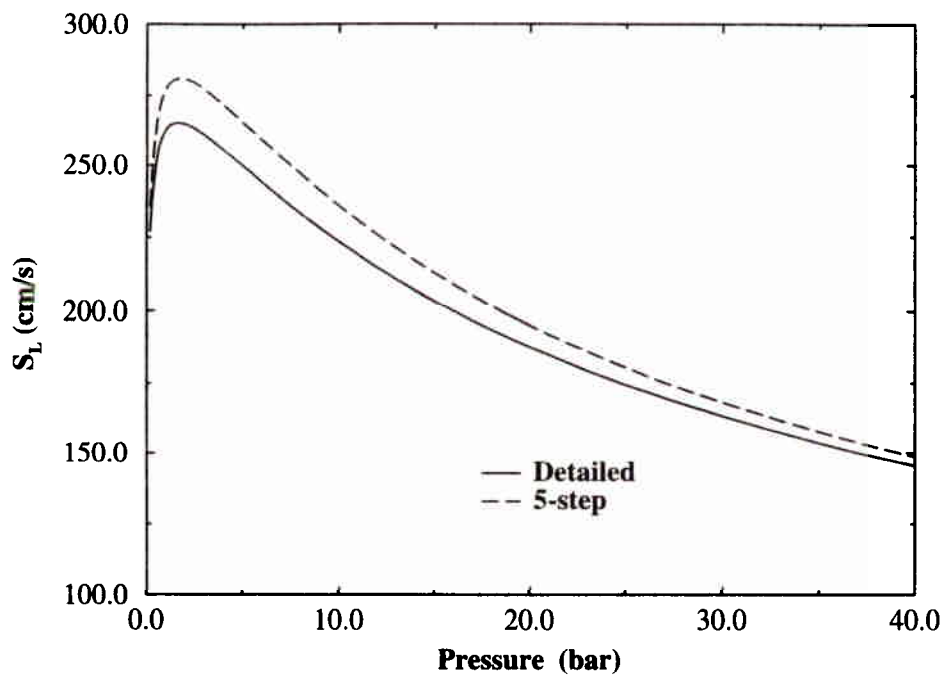


Figure 11. Laminar burning velocity as a function of pressure for hydrogen premixed flames at $\phi = 1.0$.

et al [13] shows that the inclusion of N_2O chemistry in our detailed mechanism forces CSP to choose N_2O as a major species (see section 3.1.4) and keep OH in steady state.

Figure 8 shows that the laminar burning velocity is accurately calculated for a wide range of equivalence ratios, with the reduced mechanism making a slight over-prediction around stoichiometric conditions. The flame speeds are also in good agreement with experimental data [12] (quoting Law and Warnatz), which partly validates the detailed mechanism we used. An over-prediction of the burning velocity was also evident in the two-step reduced mechanism of [12] and the discrepancy was attributed by those authors to the neglect of the steady-state species in the elemental mass balances, with the major species mass fractions taken erroneously to sum up to unity. The agreement between the reduced and detailed mechanisms was improved by *ad hoc* corrections [12], but no such effort was performed here. The NO mass fraction at the end of the domain (at $x = 30$ mm, i.e. about 28 mm from the main reaction zone) is over-predicted by about 15% (figure 9), probably due to the larger flame temperature (by about 2%) calculated by the reduced mechanism (not shown). Note that in hydrogen flames there is no prompt-NO contribution, and so the thermal mechanism, which has a high activation energy and is hence very sensitive to temperature, is the only significant one. The flame structure is captured accurately, with the profiles of major species being in very good agreement with the detailed mechanism (figure 10). Finally, figure 11 shows that the mechanism calculates laminar burning velocities accurately for pressures as high as 40 bar. The results in this section offer additional evidence of the very high accuracy that can be achieved by CSP-based reduced mechanisms. The present five-step mechanism for hydrogen premixed combustion has a wide range of validity and is of low enough dimension to be useful for turbulent flame calculations.

4. Conclusions

Two reduced mechanisms for methane–air and hydrogen–air combustion with NO formation have been constructed with the computational singular perturbation method using a previously developed fully automated algorithm. The analysis was made on solutions of unstrained adiabatic premixed flames with detailed chemical kinetics described by GRI 2.11 for methane and a 71-reaction mechanism for hydrogen that include NO_x formation. A 10-step reduced methane mechanism has been constructed which reproduces accurately flame speeds, flame temperatures and mass fraction distributions of major species for the whole flammability range. Many steady-state species are also predicted satisfactorily. It uses CH₄, O₂, H₂O, CO₂, CO, H₂, OH, H, NO, N₂O, HCNO, HCN and C₂H₂ as major species and it has been derived from a CSP analysis at $\phi = 1.2$. Comparison with our previous seven-step mechanism, which was derived at $\phi = 1.0$, shows that the improved accuracy in the calculation of C₂-species and HCN results in much better predictions for prompt NO, especially for very rich mixtures. The 10-step mechanism may also be applicable to diffusion flames. A five-step mechanism for lean and rich hydrogen combustion has been constructed based on a detailed mechanism including thermal NO, which is possibly of low enough dimensionality to be used in current PDF calculations of turbulent flames. This mechanism performs well for the whole flammable range of equivalence ratio and for pressures up to 40 bar.

The reduced mechanisms presented here were constructed with a prescribed number of global steps. This number must balance the competing needs of accuracy and simplicity of the mechanism. An algorithmic methodology for the specification of S currently does not exist and is a subject of further research.

As with past experience [33], the reduced mechanisms presented here produced CPU time savings only linear in S . The expected savings cubic in S were not realized because a very large portion of the CPU time is taken by the ‘inner iteration’ loops for the steady-state species. It is expected that other methods of computing the steady-state species will further reduce CPU time [34–36].

The mechanisms presented in this paper are all of very high accuracy. The CSP algorithm pointed to the same steady-state species as those identified by laborious analysis or intuition in the literature, but in an automatic way. In addition, the global reactions are consistent with past well established reduced mechanisms, which suggests that the CSP-based reduction method reproduces the results of the traditional way of creating reduced mechanisms. The success of the CSP-based reduced mechanisms and the algorithmic nature of CSP imply that the method is very well suited for the study of complex mechanisms of heavy hydrocarbons and for the construction of reduced mechanisms at various operating conditions.

Acknowledgments

This work has been supported by EU ESPRIT project 8835 ‘TANIT: Development of an Industrial Turbulent Combustion Code’ and the Greek Secretariat for Research and Technology through project EPET-II 649.

Appendix: Detailed mechanism for hydrogen including NO_x formation

The mechanism below is due to Yetter [27]. Elementary reaction rates are given by $k = AT^b \exp(-E/RT)$. Units are mol, cm³, mol, cal.

Table A1.

			A	b	E
1	H + O ₂ = O + OH		1.92E+14	0.0	16 440.00
2	O + H ₂ = H + OH		5.08E+04	2.7	6 292.00
3	OH + H ₂ = H + H ₂ O		2.16E+08	1.5	3 430.00
4	OH + OH = O + H ₂ O		2.10E+08	1.4	397.00
5 ^a	H ₂ + M = H + H + M		4.57E+19	-1.4	104 400.00
6 ^a	O + O + M = O ₂ + M		6.17E+15	-0.5	0.00
7 ^a	O + H + M = OH + M		4.72E+18	-1.0	0.00
8 ^a	H + OH + M = H ₂ O + M		2.25E+22	-2.0	0.00
9 ^a	H + O ₂ + M = HO ₂ + M		6.17E+19	-1.4	0.00
10	HO ₂ + H = H ₂ + O ₂		6.63E+13	0.0	2 126.00
11	HO ₂ + H = OH + OH		1.69E+14	0.0	874.00
12	HO ₂ + O = OH + O ₂		1.81E+13	0.0	-397.00
13	HO ₂ + OH = H ₂ O + O ₂		1.45E+16	-1.0	0.00
14	HO ₂ + HO ₂ = H ₂ O ₂ + O ₂		3.02E+12	0.0	1 390.00
15 ^a	H ₂ O ₂ + M = OH + OH + M		1.20E+17	0.0	45 500.00
16	H ₂ O ₂ + H = H ₂ O + OH		1.00E+13	0.0	3 590.00
17	H ₂ O ₂ + H = H ₂ + HO ₂		4.82E+13	0.0	7 948.00
18	H ₂ O ₂ + O = OH + HO ₂		9.55E+06	2.0	3 970.00
19	H ₂ O ₂ + OH = H ₂ O + HO ₂		7.00E+12	0.0	1 430.00
20	NO + M = N + O + M		1.45E+15	0.0	148 400.00
21	NO ₂ + M = NO + O + M		6.81E+14	0.0	52 800.00
22	NO + O = O ₂ + N		1.81E+09	1.0	38 750.00
23 ^b	NO + H(+M) = HNO(+M)	k_{∞}	1.52E+15	-0.4	0.00
		k_0	8.96E+19	-1.32	735.20
		$F_{\text{cent}} = 0.82$			
24	NO + H = N + OH		1.69E+14	0.0	48 800.00
25	NO + OH(+M) = HONO(+M)	k_{∞}	1.99E+12	-0.1	-7.20
		k_0	5.08E+23	-2.51	-67.56
		$F_{\text{cent}} = 0.62$			
26	NO + NO = N ₂ + O ₂		1.30E+14	0.0	75 630.00
27	NO + HO ₂ = HNO + O ₂		2.00E+11	0.0	2 000.00
28	NO ₂ + H ₂ = HONO + H		2.41E+13	0.0	28 810.00
29	NO ₂ + O = O ₂ + NO		3.91E+12	0.0	-238.40
30	NO ₂ + O(+M) = NO ₃ (+M)	k_{∞}	1.33E+13	0.0	0.00
		k_0	1.49E+28	-4.08	2 468.00
31	NO ₂ + H = NO + OH		1.29E+14	0.0	361.60
32	NO ₂ + OH(+M) = HONO ₂ (+M)	k_{∞}	2.41E+13	0.0	0.00
		k_0	6.42E+32	-5.49	2 351.00
33	NO ₂ + OH = HO ₂ + NO		1.81E+13	0.0	6 676.00
34	NO ₂ + NO = N ₂ O + O ₂		1.00E+12	0.0	60 000.00
35	NO ₂ + NO ₂ = NO ₃ + NO		9.64E+09	0.7	20 920.00
36	NO ₂ + NO ₂ = 2NO + O ₂		1.63E+12	0.0	26 120.00
37	N ₂ O(+M) = N ₂ + O(+M)	k_{∞}	1.30E+11	0.0	59 610.00
		k_0	7.23E+17	-0.73	62 780.00
38	N ₂ O + O = N ₂ + O ₂		1.02E+14	0.0	28 020.00
39	N ₂ O + O = NO + NO		6.63E+13	0.0	26 630.00
40	N ₂ O + H = N ₂ + OH		9.64E+13	0.0	15 100.00
41	N ₂ O + OH = HO ₂ + N ₂		2.00E+12	0.0	10 000.00
42	N ₂ O + NO = N ₂ + NO ₂		1.00E+14	0.0	49 675.00
43	HNO + O = OH + NO		3.61E+13	0.0	0.00
44	HNO + O = NO ₂ + H		5.00E+10	0.5	2 000.00
45	HNO + H = H ₂ + NO		1.81E+13	0.0	993.50
46	HNO + OH = H ₂ O + NO		4.82E+13	0.0	993.50

4. Conclusions

Two reduced mechanisms for methane–air and hydrogen–air combustion with NO formation have been constructed with the computational singular perturbation method using a previously developed fully automated algorithm. The analysis was made on solutions of unstrained adiabatic premixed flames with detailed chemical kinetics described by GRI 2.11 for methane and a 71-reaction mechanism for hydrogen that include NO_x formation. A 10-step reduced methane mechanism has been constructed which reproduces accurately flame speeds, flame temperatures and mass fraction distributions of major species for the whole flammability range. Many steady-state species are also predicted satisfactorily. It uses CH₄, O₂, H₂O, CO₂, CO, H₂, OH, H, NO, N₂O, HCNO, HCN and C₂H₂ as major species and it has been derived from a CSP analysis at $\phi = 1.2$. Comparison with our previous seven-step mechanism, which was derived at $\phi = 1.0$, shows that the improved accuracy in the calculation of C₂-species and HCN results in much better predictions for prompt NO, especially for very rich mixtures. The 10-step mechanism may also be applicable to diffusion flames. A five-step mechanism for lean and rich hydrogen combustion has been constructed based on a detailed mechanism including thermal NO, which is possibly of low enough dimensionality to be used in current PDF calculations of turbulent flames. This mechanism performs well for the whole flammable range of equivalence ratio and for pressures up to 40 bar.

The reduced mechanisms presented here were constructed with a prescribed number of global steps. This number must balance the competing needs of accuracy and simplicity of the mechanism. An algorithmic methodology for the specification of S currently does not exist and is a subject of further research.

As with past experience [33], the reduced mechanisms presented here produced CPU time savings only linear in S . The expected savings cubic in S were not realized because a very large portion of the CPU time is taken by the ‘inner iteration’ loops for the steady-state species. It is expected that other methods of computing the steady-state species will further reduce CPU time [34–36].

The mechanisms presented in this paper are all of very high accuracy. The CSP algorithm pointed to the same steady-state species as those identified by laborious analysis or intuition in the literature, but in an automatic way. In addition, the global reactions are consistent with past well established reduced mechanisms, which suggests that the CSP-based reduction method reproduces the results of the traditional way of creating reduced mechanisms. The success of the CSP-based reduced mechanisms and the algorithmic nature of CSP imply that the method is very well suited for the study of complex mechanisms of heavy hydrocarbons and for the construction of reduced mechanisms at various operating conditions.

Acknowledgments

This work has been supported by EU ESPRIT project 8835 ‘TANIT: Development of an Industrial Turbulent Combustion Code’ and the Greek Secretariat for Research and Technology through project EPET-II 649.

Appendix: Detailed mechanism for hydrogen including NO_x formation

The mechanism below is due to Yetter [27]. Elementary reaction rates are given by $k = AT^b \exp(-E/RT)$. Units are mol, cm³, mol, cal.

Table A1.

			A	b	E
1	H + O ₂ = O + OH		1.92E+14	0.0	16 440.00
2	O + H ₂ = H + OH		5.08E+04	2.7	6 292.00
3	OH + H ₂ = H + H ₂ O		2.16E+08	1.5	3 430.00
4	OH + OH = O + H ₂ O		2.10E+08	1.4	397.00
5 ^a	H ₂ + M = H + H + M		4.57E+19	-1.4	104 400.00
6 ^a	O + O + M = O ₂ + M		6.17E+15	-0.5	0.00
7 ^a	O + H + M = OH + M		4.72E+18	-1.0	0.00
8 ^a	H + OH + M = H ₂ O + M		2.25E+22	-2.0	0.00
9 ^a	H + O ₂ + M = HO ₂ + M		6.17E+19	-1.4	0.00
10	HO ₂ + H = H ₂ + O ₂		6.63E+13	0.0	2 126.00
11	HO ₂ + H = OH + OH		1.69E+14	0.0	874.00
12	HO ₂ + O = OH + O ₂		1.81E+13	0.0	-397.00
13	HO ₂ + OH = H ₂ O + O ₂		1.45E+16	-1.0	0.00
14	HO ₂ + HO ₂ = H ₂ O ₂ + O ₂		3.02E+12	0.0	1 390.00
15 ^a	H ₂ O ₂ + M = OH + OH + M		1.20E+17	0.0	45 500.00
16	H ₂ O ₂ + H = H ₂ O + OH		1.00E+13	0.0	3 590.00
17	H ₂ O ₂ + H = H ₂ + HO ₂		4.82E+13	0.0	7 948.00
18	H ₂ O ₂ + O = OH + HO ₂		9.55E+06	2.0	3 970.00
19	H ₂ O ₂ + OH = H ₂ O + HO ₂		7.00E+12	0.0	1 430.00
20	NO + M = N + O + M		1.45E+15	0.0	148 400.00
21	NO ₂ + M = NO + O + M		6.81E+14	0.0	52 800.00
22	NO + O = O ₂ + N		1.81E+09	1.0	38 750.00
23 ^b	NO + H(+M) = HNO(+M)	k_{∞}	1.52E+15	-0.4	0.00
		k_0	8.96E+19	-1.32	735.20
		$F_{\text{cent}} = 0.82$			
24	NO + H = N + OH		1.69E+14	0.0	48 800.00
25	NO + OH(+M) = HONO(+M)	k_{∞}	1.99E+12	-0.1	-7.20
		k_0	5.08E+23	-2.51	-67.56
		$F_{\text{cent}} = 0.62$			
26	NO + NO = N ₂ + O ₂		1.30E+14	0.0	75 630.00
27	NO + HO ₂ = HNO + O ₂		2.00E+11	0.0	2 000.00
28	NO ₂ + H ₂ = HONO + H		2.41E+13	0.0	28 810.00
29	NO ₂ + O = O ₂ + NO		3.91E+12	0.0	-238.40
30	NO ₂ + O(+M) = NO ₃ (+M)	k_{∞}	1.33E+13	0.0	0.00
		k_0	1.49E+28	-4.08	2 468.00
31	NO ₂ + H = NO + OH		1.29E+14	0.0	361.60
32	NO ₂ + OH(+M) = HONO ₂ (+M)	k_{∞}	2.41E+13	0.0	0.00
		k_0	6.42E+32	-5.49	2 351.00
33	NO ₂ + OH = HO ₂ + NO		1.81E+13	0.0	6 676.00
34	NO ₂ + NO = N ₂ O + O ₂		1.00E+12	0.0	60 000.00
35	NO ₂ + NO ₂ = NO ₃ + NO		9.64E+09	0.7	20 920.00
36	NO ₂ + NO ₂ = 2NO + O ₂		1.63E+12	0.0	26 120.00
37	N ₂ O(+M) = N ₂ + O(+M)	k_{∞}	1.30E+11	0.0	59 610.00
		k_0	7.23E+17	-0.73	62 780.00
38	N ₂ O + O = N ₂ + O ₂		1.02E+14	0.0	28 020.00
39	N ₂ O + O = NO + NO		6.63E+13	0.0	26 630.00
40	N ₂ O + H = N ₂ + OH		9.64E+13	0.0	15 100.00
41	N ₂ O + OH = HO ₂ + N ₂		2.00E+12	0.0	10 000.00
42	N ₂ O + NO = N ₂ + NO ₂		1.00E+14	0.0	49 675.00
43	HNO + O = OH + NO		3.61E+13	0.0	0.00
44	HNO + O = NO ₂ + H		5.00E+10	0.5	2 000.00
45	HNO + H = H ₂ + NO		1.81E+13	0.0	993.50
46	HNO + OH = H ₂ O + NO		4.82E+13	0.0	993.50

Table A1. Continued.

	A	b	E	
47	$\text{HNO} + \text{NO} = \text{N}_2\text{O} + \text{OH}$	2.00E+12	0.0	26 000.00
48	$\text{HNO} + \text{NO}_2 = \text{HONO} + \text{NO}$	6.02E+11	0.0	1 987.00
49	$\text{HNO} + \text{HNO} = \text{H}_2\text{O} + \text{N}_2\text{O}$	8.43E+08	0.0	3 102.00
50	$\text{HONO} + \text{O} = \text{OH} + \text{NO}_2$	1.20E+13	0.0	5 961.00
51	$\text{HONO} + \text{OH} = \text{H}_2\text{O} + \text{NO}_2$	1.26E+10	1.0	135.10
52	$\text{HONO} + \text{HNO} = \text{H}_2\text{O} + \text{NO} + \text{NO}$	1.00E+12	0.0	40 000.00
53	$\text{NH} + \text{O}_2 = \text{HNO} + \text{O}$	1.00E+13	0.0	12 000.00
54	$\text{NH} + \text{O}_2 = \text{NO} + \text{OH}$	7.60E+10	0.0	1 530.00
55	$\text{N} + \text{HO}_2 = \text{NH} + \text{O}_2$	1.00E+13	0.0	2 000.00
56	$\text{NH} + \text{O} = \text{NO} + \text{H}$	2.00E+13	0.0	0.00
57	$\text{NH} + \text{H} = \text{N} + \text{H}_2$	3.00E+13	0.0	0.00
58	$\text{N} + \text{OH} = \text{NH} + \text{O}$	3.80E+13	0.0	0.00
59	$\text{NH} + \text{OH} = \text{HNO} + \text{H}$	2.00E+13	0.0	0.00
60	$\text{NH} + \text{OH} = \text{N} + \text{H}_2\text{O}$	5.00E+11	0.5	2 000.00
61	$\text{NH} + \text{N} = \text{N}_2 + \text{H}$	1.00E+14	0.0	0.00
62	$\text{NH} + \text{NO} = \text{N}_2\text{O} + \text{H}$	2.40E+15	-0.8	0.00
63	$\text{N} + \text{HNO} = \text{NH} + \text{NO}$	1.00E+13	0.0	2 000.00
64	$\text{NH} + \text{NO}_2 = \text{NO} + \text{HNO}$	1.00E+11	0.5	4 000.00
65	$\text{N} + \text{NO} = \text{N}_2 + \text{O}$	3.27E+12	0.3	0.00
66	$\text{N} + \text{N}_2\text{O} = \text{N}_2 + \text{NO}$	1.00E+13	0.0	19 870.00
67	$\text{N} + \text{NO}_2 = \text{NO} + \text{NO}$	4.00E+12	0.0	0.00
68	$\text{N} + \text{NO}_2 = \text{N}_2\text{O} + \text{O}$	5.00E+12	0.0	0.00
69	$\text{N} + \text{NO}_2 = \text{N}_2 + \text{O}_2$	1.00E+12	0.0	0.00
70	$\text{N} + \text{HNO} = \text{N}_2\text{O} + \text{H}$	5.00E+10	0.5	3 000.00
71	$\text{HO}_2 = \text{NO} + \text{OH}$	1.00E+13	0.0	2 000.00

^a Enhanced third-body efficiencies (relative to N_2) are $[\text{M}] = 12[\text{H}_2\text{O}] + 2.5[\text{H}_2]$.

^b Pressure-dependent reaction, k_0 and k_∞ refer to low- and high-pressure limits, respectively. Reactions with specified F_{cent} parameters use the Troe form, all others use the Lindemann expression.

References

- [1] Massias A, Diamantis D, Mastorakos E and Goussis D A 1999 An algorithm for the construction of global reduced mechanisms with CSP data *Combust. Flame* to appear
- [2] Mauss F and Peters N 1993 Reduced kinetic mechanisms for premixed methane-air flames *Reduced Kinetic Mechanisms for Applications in Combustion Systems* ed N Peters and B Rogg (Berlin: Springer) p 58
- [3] Chung S H, Lee S R, Mauss F and Peters N 1993 Reduced kinetic mechanisms and NO_x formation in diffusion flames of $\text{CH}_4/\text{C}_2\text{H}_6$ mixtures *Reduced Kinetic Mechanisms for Applications in Combustion Systems* ed N Peters and B Rogg (Berlin: Springer) p 308
- [4] Bilger R W, Starner S H and Kee R J 1990 On reduced mechanisms for methane-air combustion in non-premixed flames *Combust. Flame* **80** 135
- [5] Bilger R W, Esler M B and Starner S H 1991 On reduced mechanisms for methane-air combustion *Reduced Kinetic Mechanisms and Asymptotic Approximation for Methane-Air Flames* ed M D Smooke (Berlin: Springer) p 86
- [6] Peters N and Kee R J 1987 The computation of stretched laminar methane-air diffusion flames using a reduced four-step mechanism *Combust. Flame* **68** 17
- [7] Jones W P and Lindstedt R P 1988 Global reaction schemes for hydrocarbon combustion *Combust. Flame* **73** 233
- [8] Chang W-C and Chen J-Y 1996 8-step mechanism for methane, webpage <http://firefly.berkeley.edu/griredu.html>
- [9] Chen J-Y 1997 Development of reduced mechanisms for numerical modelling of turbulent combustion *Workshop on Numerical Aspects of Reduction in Chemical Kinetics, CERMICS-ENPC (Paris)*
- [10] Smooke M D (ed) 1991 *Reduced Kinetic Mechanisms and Asymptotic Approximation for Methane-Air Flames* (Berlin: Springer)

- [11] Peters N and Rogg B 1993 *Reduced Kinetic Mechanisms for Applications in Combustion Systems* (Berlin: Springer)
- [12] Mauss F, Peters N, Rogg B and Williams F A 1993 Reduced kinetic mechanisms for premixed hydrogen flames *Reduced Kinetic Mechanisms for Applications in Combustion Systems* ed N Peters and B Rogg (Berlin: Springer) p 29
- [13] Chen J-Y, Chang W-C and Koszykowski M 1995 Numerical simulation and scaling of NO_x emissions from turbulent hydrogen jet flames with various amounts of helium dilution *Combust. Sci. Technol.* **110–111** 505
- [14] Griffiths J F 1995 Reduced kinetic models and their application to practical combustion systems *Prog. Energy Combust. Sci.* **21** 25
- [15] Seshadri K, Bollig M and Peters N 1997 Numerical and asymptotic studies of the structure of stoichiometric and lean premixed heptane flames *Combust. Flame* **108** 518
- [16] Biagioli F 1997 Comparison between presumed and Monte Carlo probability density function combustion modeling *J. Prop. Power* **13** 109
- [17] Chen J-Y and Kollamn W 1990 Chemical models for PDF modeling of hydrogen–air nonpremixed turbulent flames *Combust. Flame* **79** 75
- [18] Miller J A and Bowman C T 1989 Mechanism and modeling of nitrogen chemistry in combustion *Prog. Energy Combust. Sci.* **15** 287
- [19] Lindstedt R P, Lockwood F C and Selim M A 1995 A detailed kinetic study of ammonia oxidation *Combust. Sci. Technol.* **108** 231
- [20] Bowman C T, Hanson R K, Davidson D F, Gardiner W C, Lissianski V, Smith G P, Golden D M, Frenklach M and Goldenberg M 1996 GRI 2.11 detailed mechanism, webpage http://www.me.berkeley.edu/gri_mech/
- [21] Konnov A A 1997 Toward unified H/N/O kinetic scheme for combustion modelling *Joint Meeting of the French and Belgian Sections of the Combustion Institute* (mechanism available from webpage <http://homepages.vub.ac.be/~akonnov/science/mechanism/main.html>)
- [22] Glarborg P, Lilleheie N I, Byggstøyl S, Magnussen B F, Kilpinen P and Hupa M 1992 A reduced mechanism for nitrogen chemistry in methane combustion *24th Int. Symp. on Combustion* (Pittsburgh, PA: Combustion Institute) p 889
- [23] Hewson J C and Bollig M 1996 Reduced mechanisms for NO_x emissions from hydrocarbon diffusion flames *26th Int. Symp. on Combustion* (Pittsburgh, PA: Combustion Institute) p 2171
- [24] Goussis D A 1996 On the construction and use of reduced chemical kinetic mechanisms produced on the basis of given algebraic relations *J. Comput. Phys.* **128** 261
- [25] Rogg B 1993 Sensitivity analysis of laminar premixed CH₄–air flames using full and reduced kinetic mechanisms *Reduced Kinetic Mechanisms for Applications and Asymptotic Approximations for Methane–Air Flames* ed M Smooke (Berlin: Springer) p 159
- [26] Peters N 1990 Systematic reduction of flame kinetics: principles and details *Fluid Dynamical Aspects of Combustion Theory* ed M Onofri and A Tesei (London: Longman) p 232
- [27] Yetter R 1995 Personal communication, Princeton University
- [28] Rogg B 1993 RUN-IDL—the Cambridge universal laminar flamelet computer code *Reduced Kinetic Mechanisms for Applications in Combustion Systems* ed N Peters and B Rogg (Berlin: Springer) p 350
See also *Report CUED/A-THERMO/TR39, Department of Engineering, Cambridge University*
- [29] Turns S R 1996 *An Introduction to Combustion. Concepts and Applications* (New York: McGraw-Hill)
- [30] Warnatz J, Maas U and Dibble R W 1996 *Combustion* (Berlin: Springer)
- [31] Michaud M G, Westmoreland P R and Feitelberg A S 1992 Chemical mechanisms of NO_x formation for gas turbine conditions *24th Int. Symp. on Combustion* (Pittsburgh, PA: Combustion Institute) p 879
- [32] Lindstedt R P and Selim M A 1994 Reduced reaction mechanisms for ammonia oxidation in premixed laminar flames *Combust. Sci. Technol.* **99** 277
- [33] Somers L M T and DeGoeij L P H 1994 Analysis of systematic reduction technique *25th Int. Symp. on Combustion* (Pittsburgh, PA: Combustion Institute) p 957
- [34] Turanyi T 1994 Parametrization of reaction mechanisms using orthogonal polynomials *J. Comput. Chem.* **18** 45
- [35] Pope S B 1997 Computationally efficient implementation of combustion using *in situ* adaptive tabulation *Combust. Theory Modelling* **1** 41
- [36] Niemann H, Schmidt D and Mass U 1997 An efficient storage scheme for reduced chemical kinetics based on orthogonal polynomials *J. Engng Math.* **31** 131–42